Turbulent dynamics of an intrinsically chaotic field

Farid F. Abraham
IBM Research Division, Almaden Research Center, 650 Harry Road, San Jose, California 95120-6099
(Received 8 November 1993)

We have simulated the nonlinear dynamics of a two-dimensional lattice of damped-driven oscillators where the dynamical state of the isolated individual oscillator is chaotic. Harmonic coupling between these oscillators results in a very rich and complex spatiotemporal dynamics as a function of coupling strength. The dynamics is characterized by coherent clusters of energy moving randomly in a structureless background, growing in size with increasing coupling, and undergoing a sequence of "freezing transitions" until a coupling is reached where a single cluster dominates the lattice extent. The intricate interplay of coherent and random dynamics suggests a possible analogy with high Reynolds number turbulent flow. Extended self-similarity proposed for turbulent flows and applied to this problem indicates a universality in the dynamics. This suggests that the extension to other (more realistic) representations of physical systems may provide a fruitful paradigm for studying dynamical disorder in the real world.

PACS number(s): 05.45.+b

A lattice of interacting point particles is a paradigm from which we have learned about certain limited dynamical behavior that occurs in many-body systems. From this idealized model, a more general picture has evolved of a dynamical system defined by an assembly of a large number of identical subsystems of known intrinsic dynamics that are coupled to each other in some specific manner [1,2]. The general goal is to study the global dynamical behavior of the total system on the basis of the known nature of the subsystem and the coupling between a large number of subsystems. We recently studied an application of this synthetic view of a dynamical system by allowing a much richer intrinsic behavior of the elementary subsystem [3]; in particular, we considered the dynamics of the "independent" subsystem to be chaotic, instead of a point-atom or a simpler limit-cycle oscillator. For a linear chain of chaotic oscillators, we discovered that harmonic lattice coupling gave rise to a complex and rich spatiotemporal many-body dynamics as a function of coupling strength. This present study extends this model to two dimensions, and the higher dimension results in entirely different spatiotemporal dynamics. We will show that this new dynamics has much similarity with real fluid turbulence.

We make no attempt to model "fluid" turbulence. Instead, we consider a "mechanical model of turbulence" where a mesoscopic approximation takes the turbulent subsystems as chaotic oscillators, which are coupled harmonically on a two-dimensional square lattice. For the chaotic oscillator, we adopt the damped-driven pendulum [4]. The dynamical equation is the second-order differential equation,

$$\frac{d^2\phi}{dt^2}=-\alpha\frac{d\phi}{dt}-\omega_0^2\sin(\phi)+A\cos(\omega t)\ , \tag{1}$$

where ϕ is the displacement, α is the damping factor, ω_0 is the natural oscillation frequency, and ω and A are the frequency and amplitude of the external torque. This subsystem can operate in far-from-equilibrium situations so that it represents a very active functional subunit of the total system. We choose the following values for the parameters which give a chaotic state of the isolated oscillator: $\omega_0=2.53$, $\alpha=0.25$, $\omega=1.62$, $A=3.8$. These parameters are not changed in our study. Our total dynamical system is a square array of these oscillators coupled harmonically in ϕ with a coupling constant κ. The force $F_\kappa(k)$ at the i,j lattice site due to neighboring oscillators is

$$F_\kappa(i,j)=\kappa[\phi(i+1,j)+\phi(i-1,j)-2\phi(i,j)+\phi(i,j+1)+\phi(i,j-1)-2\phi(i,j)]\ . \tag{2}$$

The initial angles and velocities are taken to be random, and periodic boundary conditions are imposed at the border of the $L\times L$ square lattice. We note two obvious dynamical features of this system: for $\kappa=0$, we have $N=L\times L$ independent chaotic oscillators, and for $\kappa\gg1$, we have one "large" chaotic oscillator. We are interested in discovering what is between zero coupling and infinite coupling; hence the many-body physics of coupled chaotic oscillators. We have studied the system dynamics as a function of lattice size L and coupling constant κ. We found that the steady-state dynamical behavior was scale invariant with respect to the relationship $\kappa=\text{const}\times L^2$. This can be understood by approximating our dynamical equations by the partial differential equation (the damped-driven sine-Gordon equation),

$$\frac{\partial^2\phi}{\partial t^2}=\beta\frac{\partial^2\phi}{\partial x^2}+\beta\frac{\partial^2\phi}{\partial y^2}-\alpha\frac{\partial\phi}{\partial t}-\omega_0^2\sin(\phi)+A\cos(\omega t)\ , \tag{3}$$

where $\beta=a^2\kappa$ and a is the lattice spacing in approximating Eq. (2) by a second-order partial derivative. If the characteristic features of the dynamics scale with the length of the chain $L=aN$, then from Eq. (3) we conclude that $\beta/L^2=a/L^2\kappa=\text{const}$. Therefore, the scale-invariant dynamics satisfies the relation $\kappa=\text{const}\times L^2$. The system sizes ranged from $L=16$ to 128, but most simulations were based on $L=61$ and 64.

Instead of measuring the continuous temporal evolution of the vibrations of the oscillators at each lattice site, we record discrete displacements and velocities at each Poincaré cycle. This mathematical technique simplifies the complicated dynamics by viewing the trajectory stroboscopically, the strobe period being equal to the forcing period of the individual oscillators. Hence, time flows in discrete units of the strobe period and strobe dynamic images (SDI) are segmented jumps in displacement and velocity. For purposes of visualization, we chose kinetic energy, or velocity squared, to represent the local instantaneous dynamical feature of the oscillator at each lattice site, which is color coded on a scale of 1 to 6 (hence, "chromodynamics of SDI"). The advantage of viewing the temporal sequence of these images becomes apparent when we consider the "motion picture" of the collective lattice dynamics of our system. For periodic motion, there are a finite number of distinct SDI's, equal to the Poincaré period, and the image sequence repeats. For period 1 we see one static image, while for chaotic motion the chromodynamics of SDI's will be "noisy" with no time periodicity. In this paper, it is only possible to display a "hint" of the complex pattern dynamics obtained using this graphical analysis technique. We will show a time sequence of a few SDI snapshots in hopes of capturing the temporal pattern change, but a movie is essential. Observing the chromodynamics of the SDI was crucial to the interpretation of the experiments, much like the need for visualizing turbulent fluid flow.

In Figs. 1–4, a time sequence of three SDI snapshots is presented as a row for each coupling parameter κ. The time interval between snapshots for a given row is constant and arbitrarily chosen so as to give an indication of the pattern dynamics for a given coupling. In Fig. 1, we see that as κ increases from zero (no coupling, hence independently vibrating chaotic oscillators) to thirty, localized "clusters of high kinetic energy" (red and yellow) in a low kinetic-energy background (greens and blue) be-

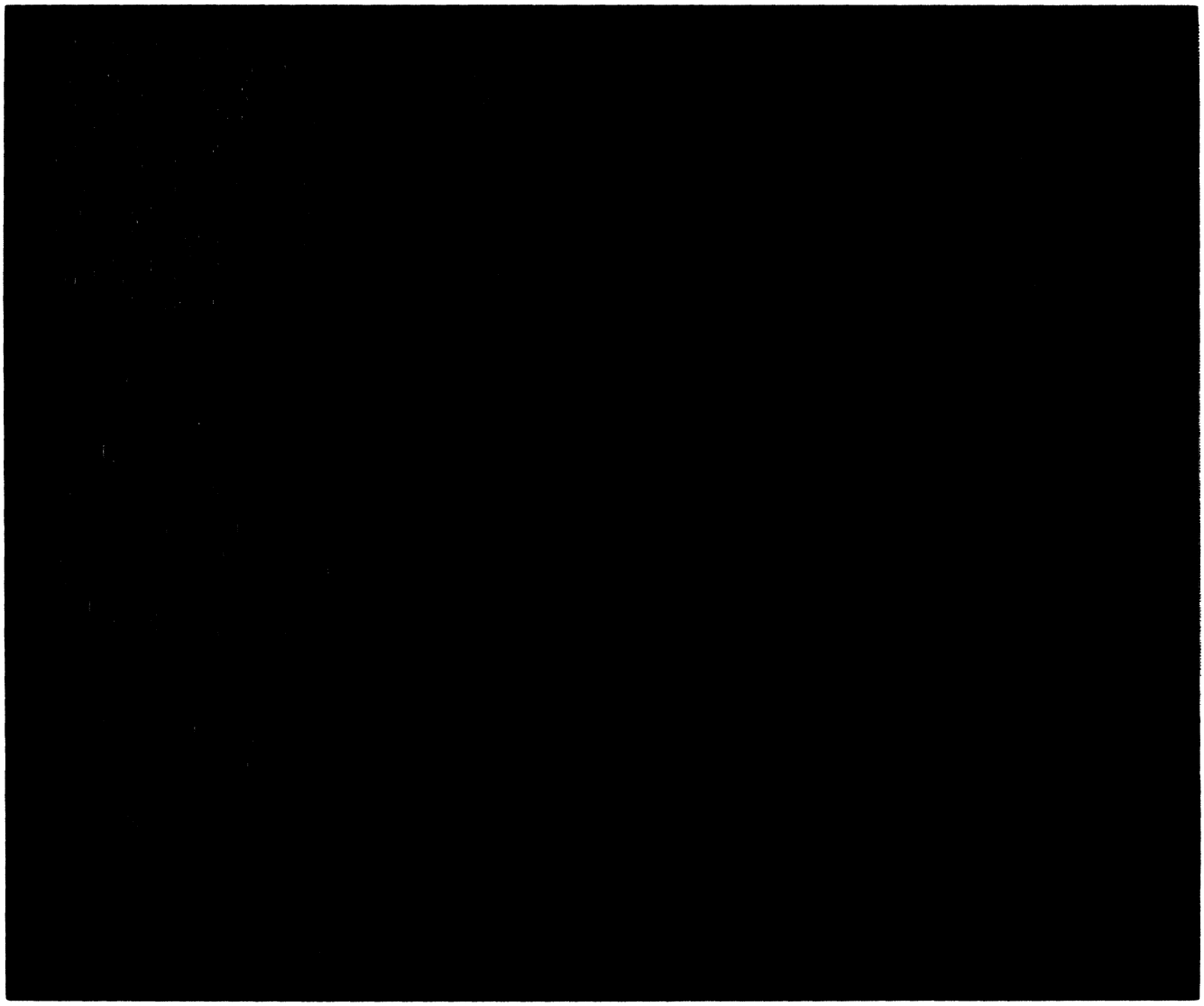

FIG. 1. Successive rows of SDI snapshots from top to bottom are for $\kappa=0,20,30$.

come prevalent. The clusters have a compact, but rough, structure that increases in average size with increase κ. The apparent motion is quite erratic, much like a "liquid of Brownian clusters randomly walking and interacting in two-dimensional space"; i.e., we see clumps of intense turbulence energy in a relatively quiescent background. Of course, no cluster of energy remains constant in size or in existence throughout the simulation. In Fig. 2, the successive rows of SDI snapshots from top to bottom are for $\kappa=40$, 60, and 80. For $\kappa=40$, the kinetic energy pattern "crystallizes" into a square lattice of four clusters per computational cell, but the crystal pattern is unstable and fluctuates between a "liquid state" and "crystal state," as suggested by the different unit cell configurations displayed. For $\kappa=60$, we returned to the liquid state with larger average size cluster. At $\kappa=80$, the systems again crystallizes, but now with two clusters per unit computational cell and with the average cluster size being approximately twice the value for $\kappa=40$. These features are demonstrated in Fig. 5(a) where the cluster size distribution is plotted for the three couplings (we arbitrarily define a cluster as a connected red-yellow region in the instantaneous color field for the kinetic energy) and in Fig. 5(b) where the instantaneous average kinetic energy as a function of time is plotted for these same couplings. We note that the crystal state is much more stable at $\kappa=80$, suggesting that there exists a unique κ for an infinite-lifetime crystal state and that we are closer to that value for the two clusters per unit cell ($\kappa=80$) than for the four clusters per unit cell ($\kappa=40$). Simulations for $\delta\kappa=1.0$ changes around $\kappa=40$ and 80 show that there is a much larger window for quasistability for $\kappa=80$ and that the small scale fluctuations, on the size of a lattice spacing, is preventing long-life stability when the cluster size is not sufficiently larger than the lattice scale. We verified this by studying smaller two-dimensional arrays but did not quantify this behavior. In Figs. 3 and 4, the successive rows of SDI snapshots from

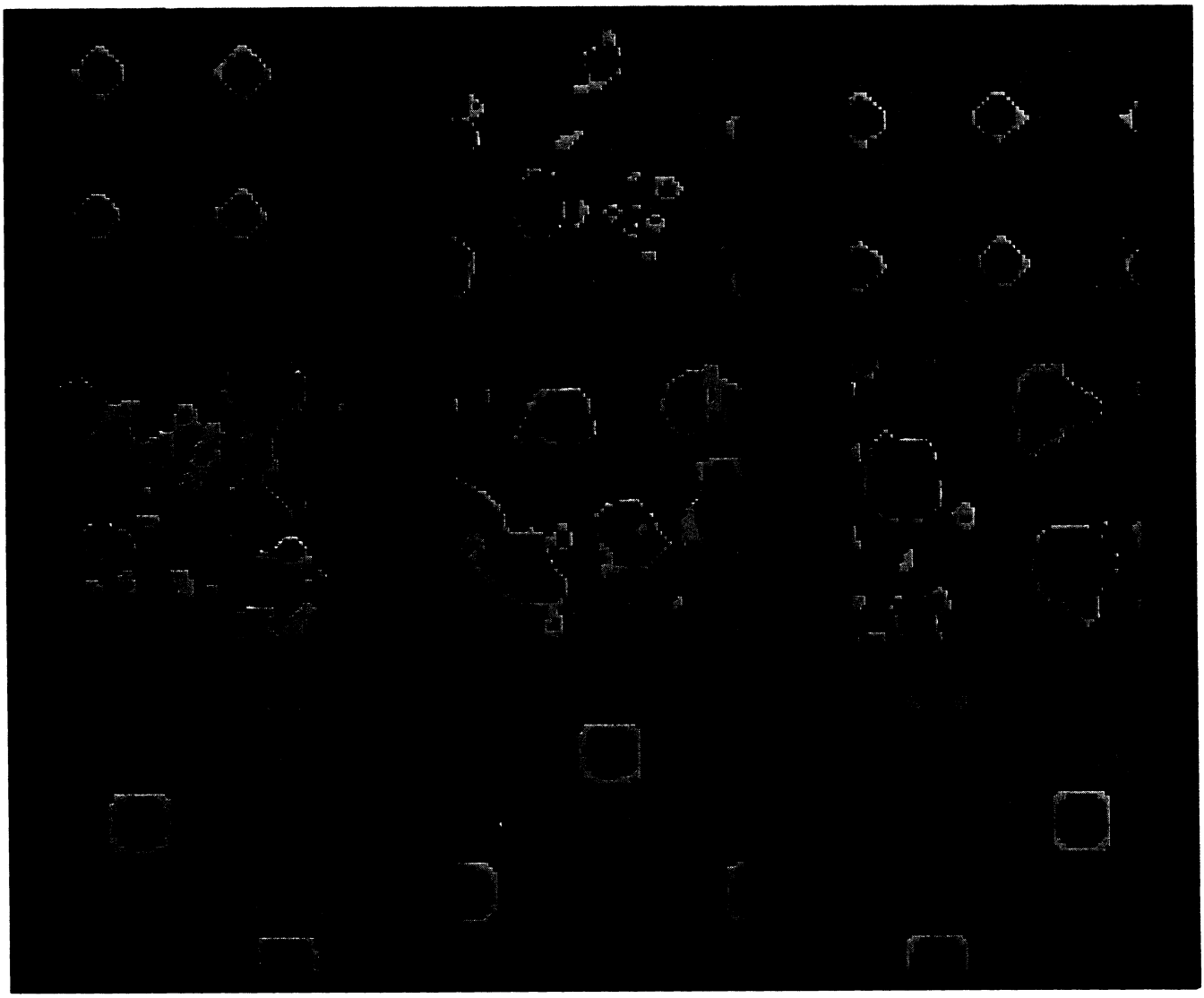

FIG. 2. Successive rows of SDI snapshots from top to bottom are for $\kappa=40,60,80$.

top to bottom are for $\kappa=90,100,110,120,135,300$. We see that at $\kappa=135$, the system has again crystallized, but now with one cluster per computational cell. For simulation times up to 10 000 cycles, the field was stable. The cluster size is again approximately twice the value for previous $\kappa=80$. Between the two crystal points, $\kappa=80$ and $\kappa=135$, the SDI's no longer have the appearance of a turbulent liquid. Instead, the spatial patterns have significant symmetry, while always changing and sometimes repeating. The variety of patterns appears to be inexhaustible. The last row of SDI's is for $\kappa=300$, and represents a cluster pulsating in size at the Poincaré period. For infinite coupling, we would observe a solid color field changing colors erratically. The peak and average cluster sizes as a function of coupling strength have been calculated from the size distributions [e.g., see Fig. 5(a)], and an excellent linear dependence is found. To summarize, we observe the kinetic energy pattern to crystallize into a square lattice of four clusters per computational cell at $\kappa=40$, two clusters per computational cell at $\kappa=80$, and one stable cluster per computational cell at $\kappa=135$, each respective cluster size being approximately twice the value of the previous κ. Each frozen pattern is representative of spatial periodic dynamics with period 1.

Returning to the lower couplings κ, we noted the apparent mixture of clustered erratic motion in a two-dimensional calm background. Ruelle, in his remarkable book entitled *Chance and Chaos,* points out that most approximate theories of fluid turbulence assume that turbulence is homogeneous while turbulence is actually spatially and temporally inhomogeneous with the coexistence of fluctuating regions of smooth and erratic dynamics [5]: "In reality, a turbulent fluid always shows clumps of intense turbulence in a relatively quiescent background. And hydrodynamicists keep looking for the correct theory to describe this clumpiness." This fact was reemphasized by Smith and Yakhot [6] in an extraor-

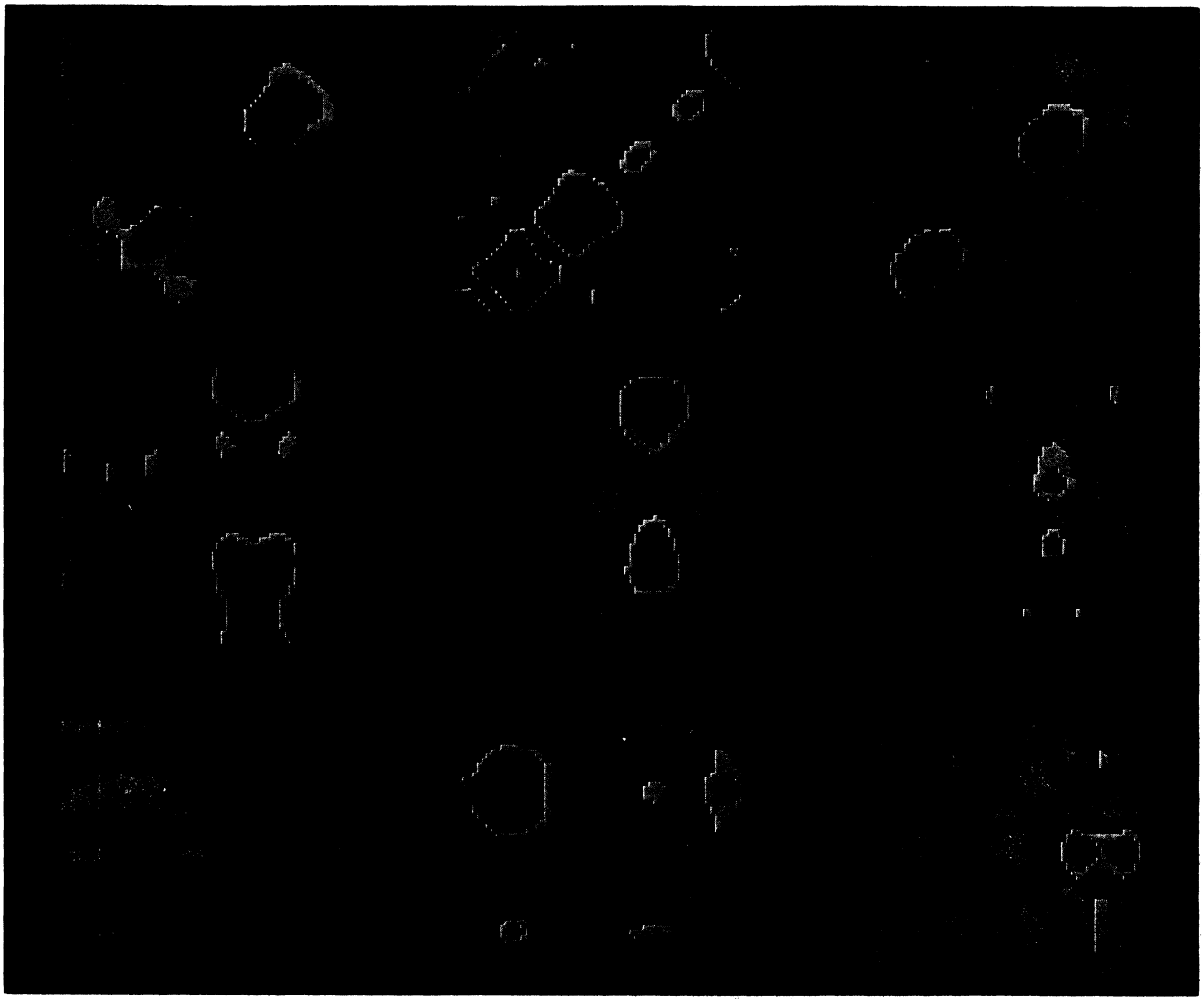

FIG. 3. Successive rows of SDI snapshots from top to bottom are for $\kappa=90,100,110$.

dinary simulation study on two-dimensional turbulence where they state: "High Reynolds number turbulent flows are characterized by complexity, loosely defined as an intricate interplay of coherent and random dynamics." In the context of trying to understand the global dynamical behavior of our model, the previous remarks motivated us to consider our system to be in a "turbulent" state and to see how similar it is to "real" fluid turbulence.

Benzi *et al.* [7] have established a new form of self-similarity in turbulent flows which they named extended self-similarity (ESS). Defining $\Delta V(r)=V(x+r)-V(x)$, where $V(x+r)$ and $V(x)$ are velocities along the x axis separated by a distance r, they considered the expression

$$G_n=\langle\langle\,|\Delta V(r)|^n\rangle\rangle=B_n\langle\langle\,|\delta V(r)|^3\rangle\rangle^{\zeta(n)}\,, \tag{4}$$

where $\langle\langle\ \rangle\rangle$ denotes averaging. They found that the scaling exponents $\zeta(n)$ agree with the exponents of fully developed turbulence obtained from the relationship

$$\langle\langle\,[\Delta V(r)]^n\rangle\rangle\sim r^{\zeta(n)}\,, \tag{5}$$

where $\nu\ll r\ll L$, L being the integral scale of motion and ν being the dissipative scale. Furthermore, Benzi *et al.* claim that Eq. (4) is valid not only for fully developed turbulence but also for moderate Reynolds number. The Kolmogorov theory predicts $\zeta(n)=n/3$. We have performed the ESS analysis for our chaotic oscillator field for couplings that appear turbulent, and the results are shown in Figs. 6(a) and 6(b). Our Fig. 6(a) is to be compared to Benzi's Fig. 3(a) where a log-log plot of $G_2=\langle\langle\,|\Delta V(r)|^2\rangle\rangle$ vs $G_3=\langle\langle\,|\Delta V(r)|^3\rangle\rangle$ is presented for "real fluid" flow past a cylinder at Reynolds numbers 6000 and 47 000. The slope and intercept for the two plots are identical. In Fig. 6(b), the scaling exponents $\zeta(n)$ computed for $n=1$ to 6 (the dots) are presented and compared with the fluid turbulence measurements of Benzi *et al.* [7] (the diamonds) and the Kolmogorov theory. Again, we note good agreement with our model

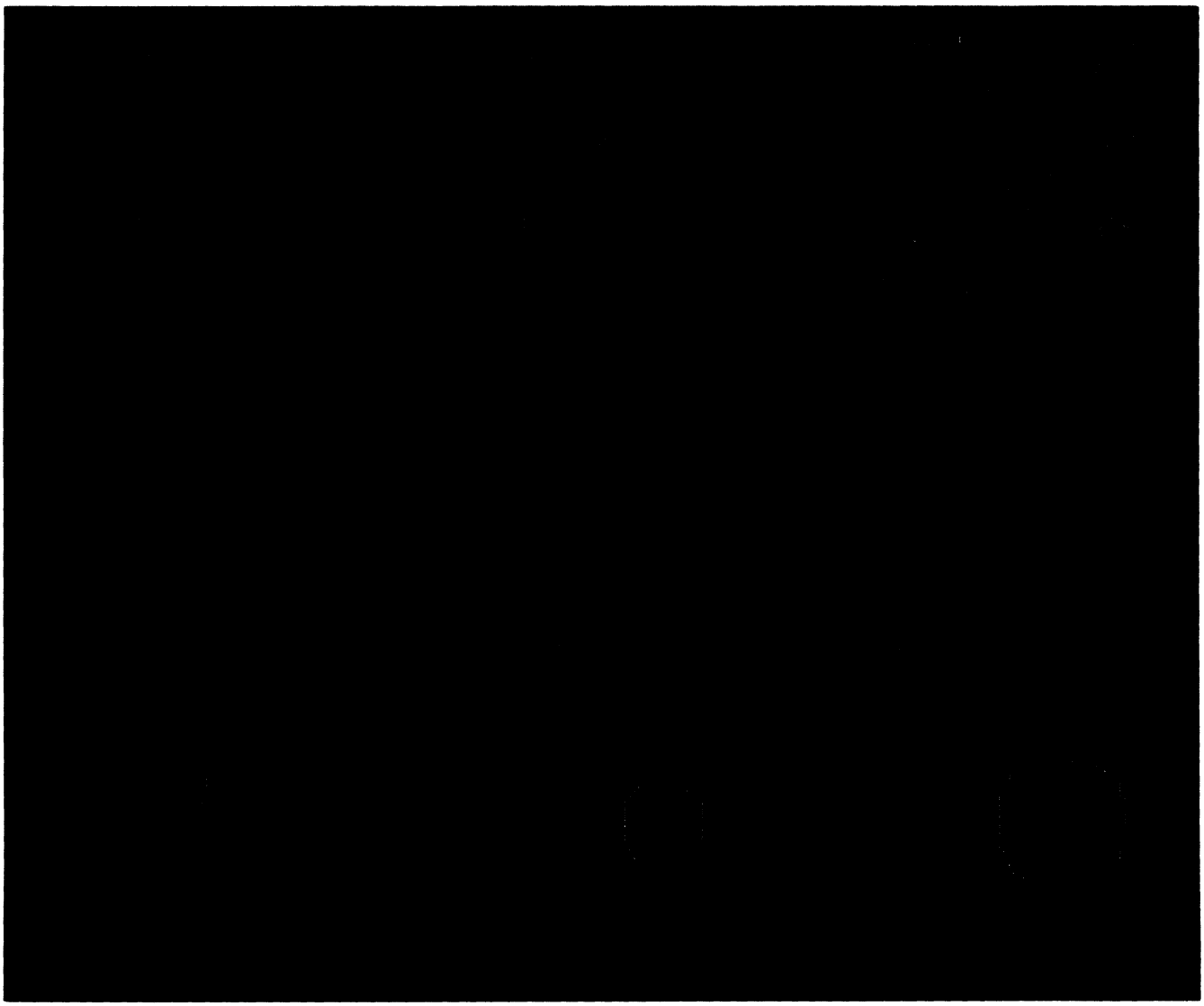

FIG. 4. Successive rows of SDI snapshots from top to bottom are for $\kappa=120,135,300$.

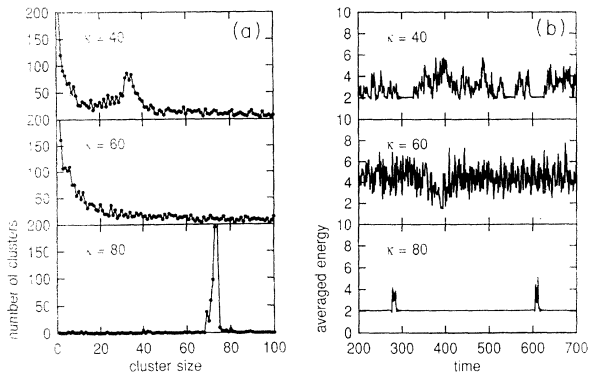

FIG. 5. (a) The cluster distribution as a function of size is plotted for the coupling $\kappa=40,60,80$ (we arbitrarily define a cluster as a connected red-yellow region in the instantaneous color field for the kinetic energy). (b) The instantaneous average kinetic energy as a function of time is plotted for $\kappa=40,60,80$. The time unit is equal to the forcing period (or Poincaré period) of the individual oscillator.

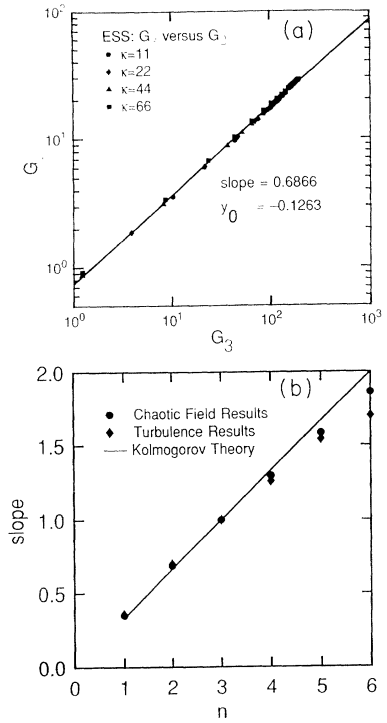

FIG. 6. (a) Log-log plot of $G_2=\langle\langle|\Delta V(r)|^2\rangle\rangle$ vs $G_3=\langle\langle|\Delta V(r)|^3\rangle\rangle$ is presented for the denoted couplings corresponding to the "turbulent" states of the chaotic oscillators field. (b) The scaling exponents $\zeta(n)$ computed for $n=1, 2, 3, 4, 5$, and 6 (the dots) and compared with the fluid turbulence measurements of Benzi *et al.* [7] (the diamonds) and the Kolmogorov theory.

and real fluid turbulence. This suggests a universality in the "turbulence" dynamics of a real fluid and our chaotic oscillator field. In the context of trying to understand this global turbulent behavior, we think of our system as a coarse-grain dynamical model where each subsystem is turbulent when in isolation and the total system dynamics arises from intersubsystem coupling; i.e., the intrinsic "homogeneous turbulence" of the collective subcells gives rise to a global dynamical structure that is not uniformly turbulent in space and time. A detailed ESS analysis between fluid and oscillator turbulence is in progress [8].

We have learned that this simple model of coupled, "intrinsically" chaotic subsystems can exhibit a very rich and complex dynamics, both in space and time. Of course, the obvious impulse is to study larger systems, different types of chaotic subsystems, various local and nonlocal coupling schemes, higher dimension packings, mixed systems (chaotic and periodic subsystems), frustration, and much more. However, the very simple concept of modeling the interaction of chaotic subsystems may provide a new paradigm for studying spaciotemporal turbulence in the real world.

The author thanks Dr. Sauro Succi for bringing Ref. [7] to his attention.

[1] R. Z. Sagdeev, D. A. Usikov, and G. M. Zaslavsky, *Nonlinear Physics: From the Pendulum to Turbulence* (Harwood Academic, Chur, Switzerland, 1988).

[2] E. Atlee Jackson, *Perspectives of Nonlinear Dynamics: I and II* (Cambridge University Press, Cambridge, England, 1991).

[3] F. F. Abraham, Phys. Rev. E **47**, 1625 (1993).

[4] G. L. Baker and J. P. Gollub, *Chaotic Dynamics: An Introduction* (Cambridge University Press, Cambridge, England, 1990).

[5] D. Ruelle, *Chance and Chaos* (Princeton University Press, Princeton, NJ, 1991).

[6] L. M. Smith and V. Yakhot, Phys. Rev. Lett. **71**, 352 (1993).

[7] R. Benzi, S. Ciliberto, R. Tripiccione, C. Baudet, F. Massaioli, and S. Succi, Phys. Rev. E **48**, R29 (1993).

[8] F. F. Abraham and S. Succi (unpublished).

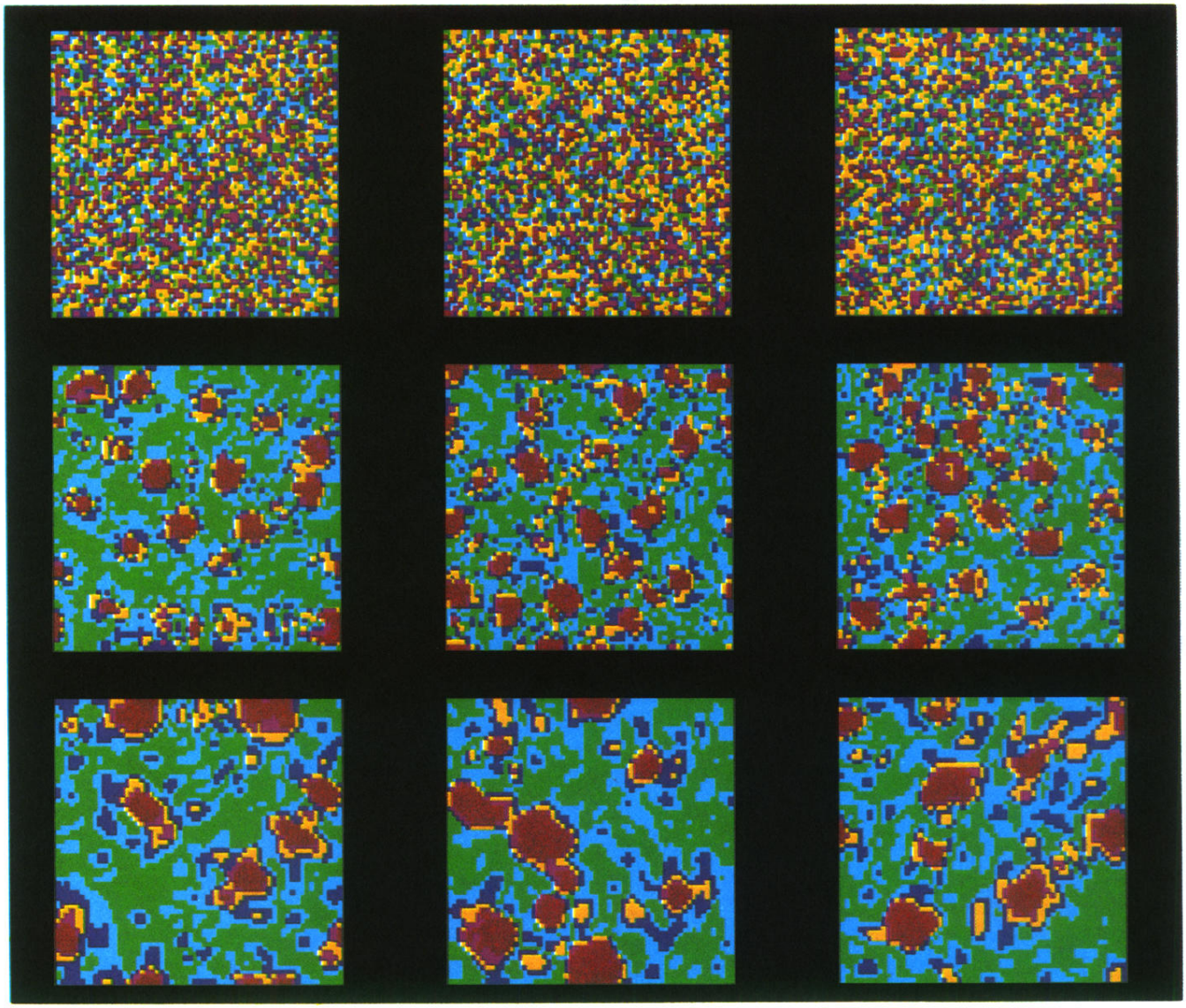

FIG. 1. Successive rows of SDI snapshots from top to bottom are for $\kappa=0,20,30$.

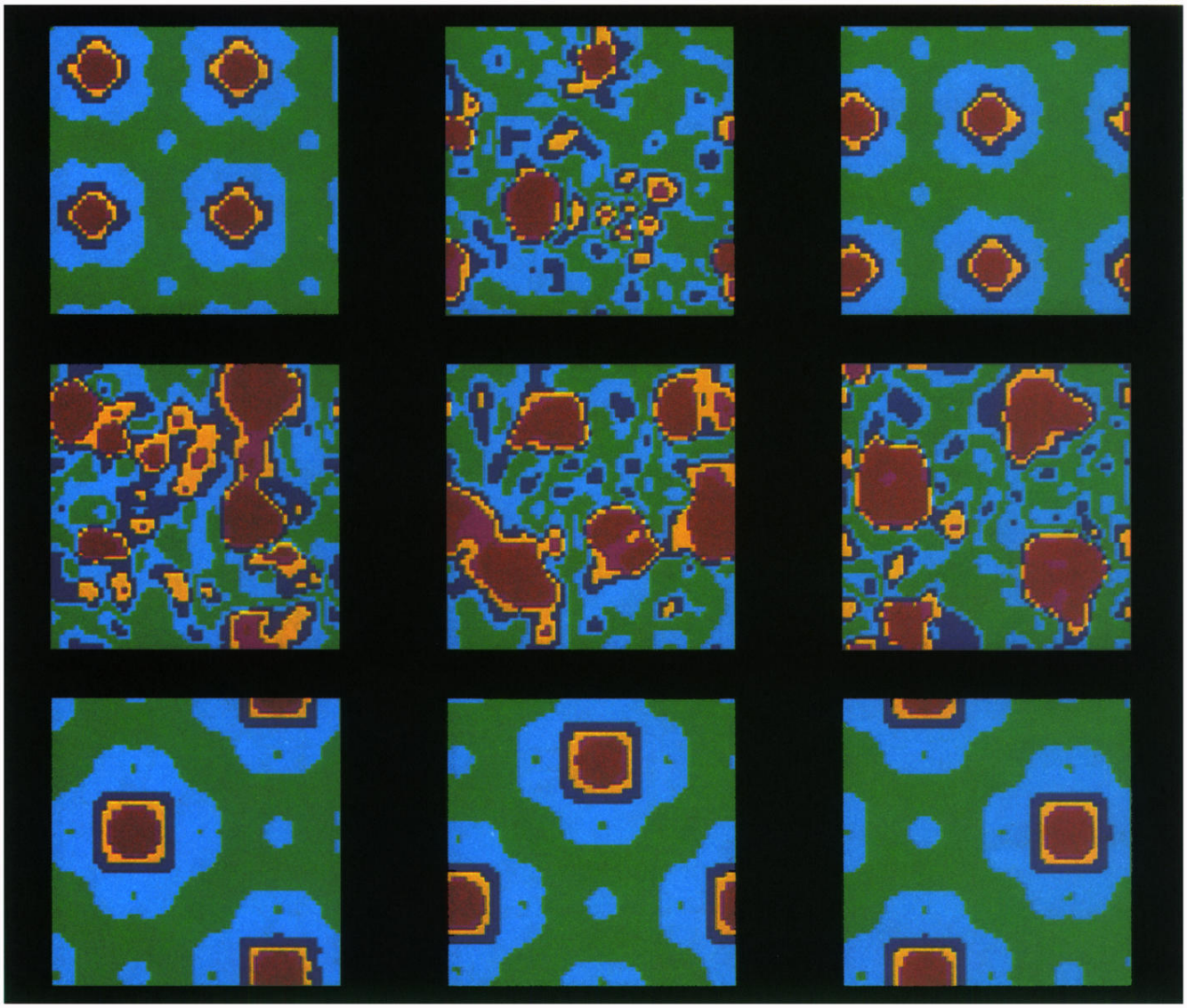

FIG. 2. Successive rows of SDI snapshots from top to bottom are for $\kappa = 40, 60, 80$.

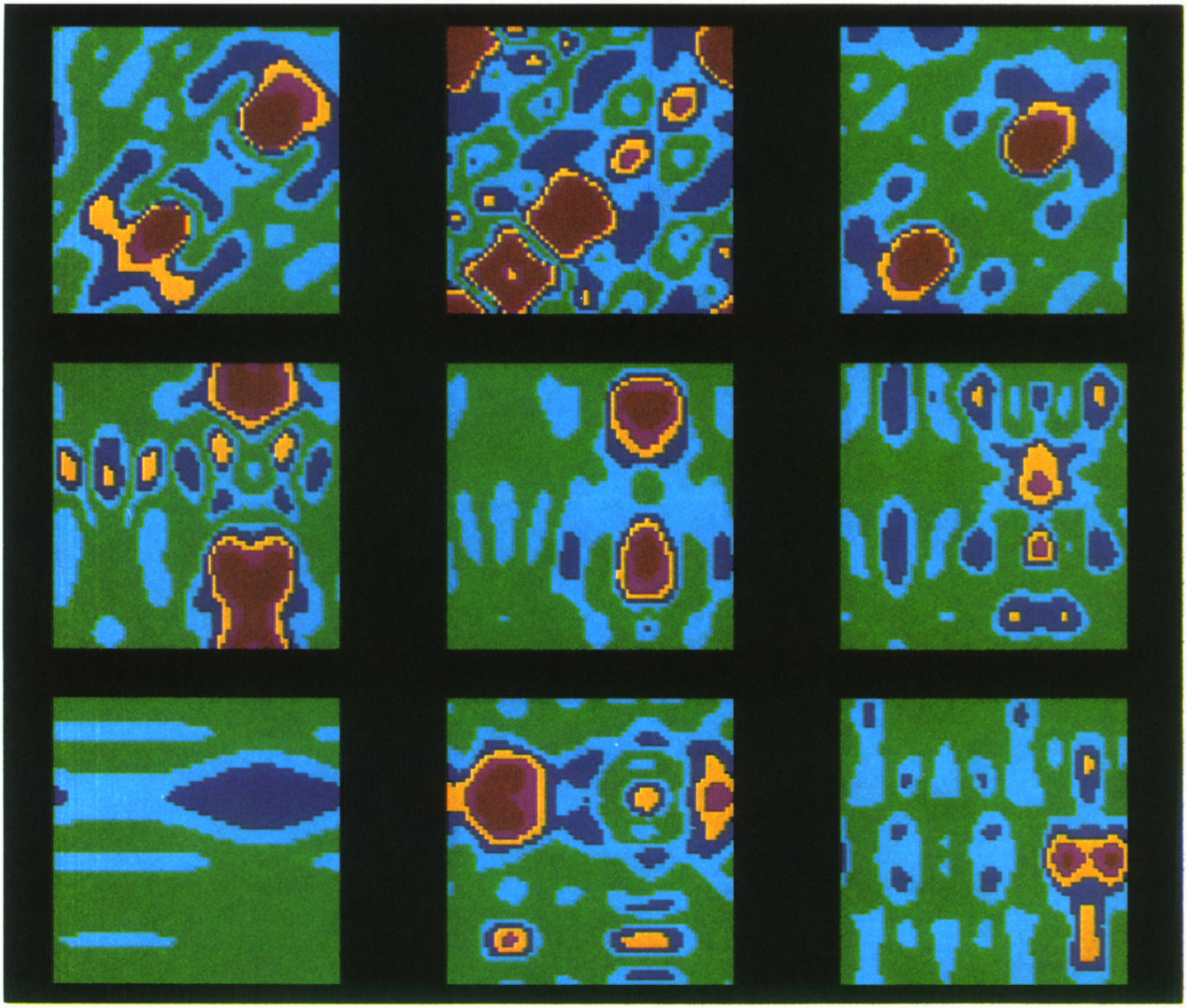

FIG. 3. Successive rows of SDI snapshots from top to bottom are for $\kappa = 90, 100, 110$.

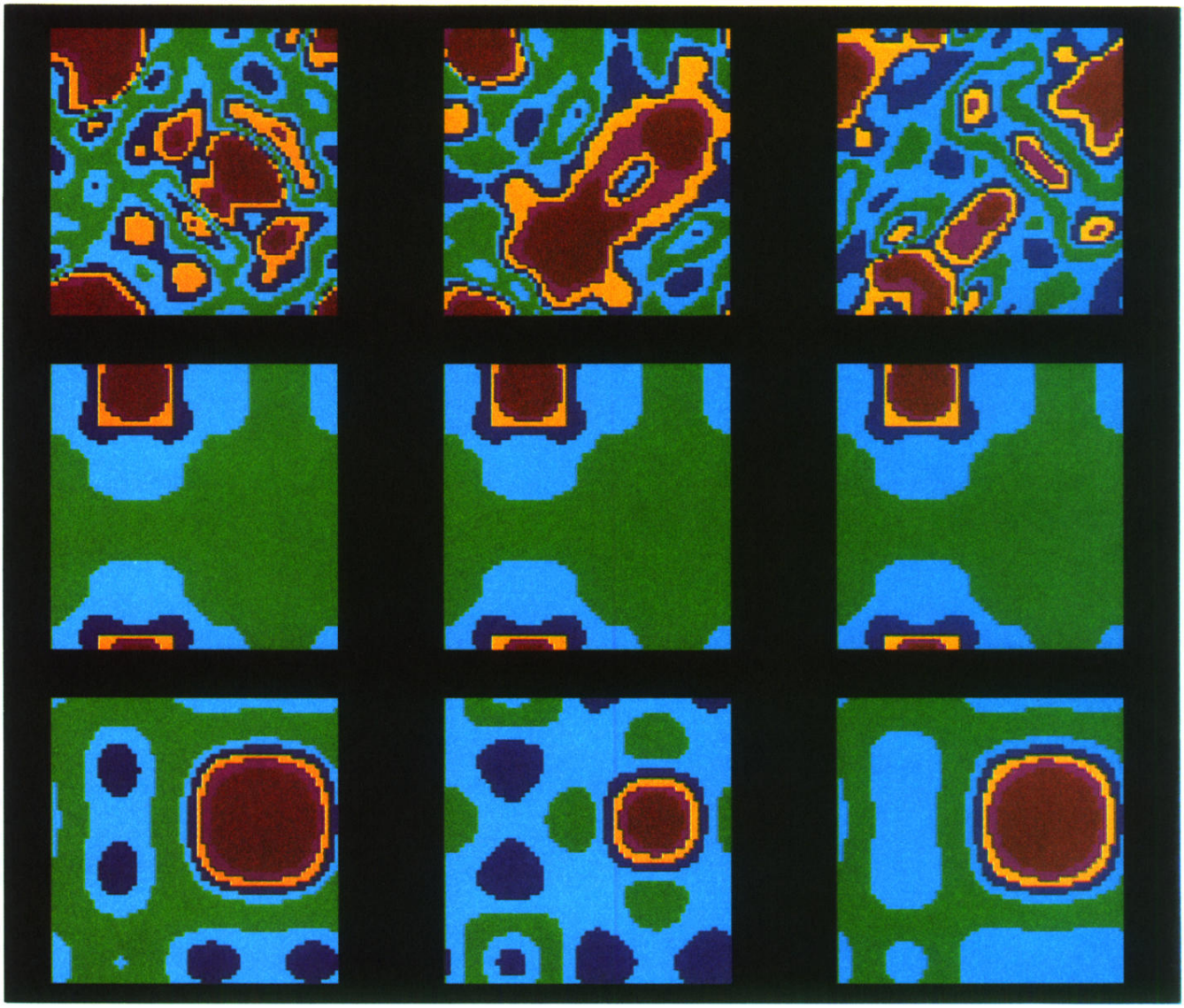

FIG. 4. Successive rows of SDI snapshots from top to bottom are for $\kappa = 120, 135, 300$.